Available online at www.sciencedirect.com
SCIENCE DIRECT
Journal of Molecular Catalysis A: Chemical 243 (2006) 204–213
JOURNAL OF MOLECULAR CATALYSIS A: CHEMICAL
www.elsevier.com/locate/molcata

Promoting effect of ceria on the physicochemical and catalytic properties of CeO_2–ZnO composite oxide catalysts

Braja Gopal Mishra, G. Ranga Rao *

Department of Chemistry, Indian Institute of Technology Madras, Chennai 600036, India

Received 2 May 2005; received in revised form 30 July 2005; accepted 30 July 2005
Available online 23 September 2005

Abstract

CeO_2–ZnO composite catalysts prepared by amorphous citrate method have been investigated for cyclohexanol dehydrogenation and hydrogen transfer reactions. The precursors and catalysts have been characterized by TGA, CHN analysis, XRD, UV–vis–NIR diffuse reflectance, SEM and acid–base measurements. The amorphous precursors in citrate process contain one molecule of citric acid per Ce^{4+} or Zn^{2+} ions. Structural studies of composite oxides indicate the presence of individual oxide phases along with non-equilibrium solid solutions in a limited composition range. The composite oxides contain low coordination Ce^{3+} and Ce^{4+} sites. Cyclohexanone was obtained as main product for cyclohexanol transformation reaction carried out over these mixed oxide catalysts due to dehydrogenation on basic sites. The presence of ceria in the composite oxide enhances the surface area and acid–base properties facilitating the dehydrogenation process. At low ceria content, the CeO_2–ZnO composite oxide catalysts show higher catalytic activity for both cyclohexanol dehydrogenation and hydrogen transfer reactions due to higher basicity, surface area and smaller crystallite sizes. Hydrogen transfer activity is found to be higher on CeO_2(10%)–ZnO catalyst prepared by citrate method compared to the catalyst prepared by decomposition from acetate precursor. This study demonstrates the promoting effect of ceria in CeO_2–ZnO catalysts for reactions involving acid–base sites.

Keywords: CeO_2; ZnO; CeO_2–ZnO; UV–vis–DRS; Cyclohexanol transformation; Hydrogen transfer reaction

1. Introduction

Ceria and ceria-based composite oxide systems have been extensively investigated for catalytic applications such as three-way catalysis, catalytic wet oxidation, water–gas-shift reaction, oxidation/combustion catalysis and solid oxide fuel cells [1–7]. The redox property of ceria plays a prominent role in all these catalyzed reactions. The number of effective redox sites and their ability to exchange oxygen can be manipulated by incorporating transition metal ions into the ceria lattice and promoted by noble metals dispersed on ceria [1,7–10]. Zirconia-incorporated ceria is a good example which shows enhanced reducibility in the presence of noble metals such as Rh, Pt and Pd [11–14]. While the role of ceria has been well established as a redox promoter, there is much scope to investigate the acid–base properties of ceria-based materials. Ceria-based composite oxides have been increasingly studied for their role as acid–base catalyst/promoter for various reactions. The promoting/catalyzing effect of ceria in pure or in the form of composite oxide is attributed to the combination of acid–base and redox properties of ceria. Addition of ceria into MgO has been found to increase the number of effective weak base sites responsible for alkylation reaction [15,16]. Similarly, in the case of CeO_2–CaO composite system, the surface acid–base property is found to increase at low ceria content and the effect is more prominent on acidic sites [17]. The acid–base property of ceria and ceria-based composite oxide materials have been studied by microcalorimetry [18,19], in situ IR study of adsorbed pyridine and CO_2 [20] and model reactions [21]. These studies generally agree that the surface acidic property is due to surface Ce^{4+} and $OH^{\delta+}$ species while the basic property is related to surface O^{2-} and $OH^{\delta-}$ ions [20]. The relative amounts of surface unsaturated cations and the hydroxyl groups contributing to acid–base sites depend on the method of preparation. Sato et al. [15] showed that ceria samples prepared from different precursor salts show different surface areas, acid–base

* Corresponding author. Tel.: +91 44 2257 4226; fax: +91 44 2257 4202.
E-mail address: grrao@iitm.ac.in (G.R. Rao).

1381-1169/$ – see front matter © 2005 Elsevier B.V. All rights reserved.
doi:10.1016/j.molcata.2005.07.048

properties and catalytic activity for alkylation of phenol. Martin and Duprez [21] have shown the presence of strong basic sites on ceria and correlated them with oxygen mobility [22]. Microcalorimetric measurements on ceria surface indicate the presence of strong basic sites which are not homogenously distributed. Doping small amount of zirconium in the ceria lattice remarkably modifies the basic character of the solid solution. The $Ce_{0.8}Zr_{0.2}O_2$ phase is reported to exhibit high heat of CO_2 adsorption and homogeneous basic sites [19]. It is therefore clear that the surface properties and catalytic activity of ceria can be improved by synthesizing appropriate ceria-based composite oxides.

The $Ce_{1-x}Zn_xO_{2-x}$ ($x = 0$–0.56) solid solutions prepared by soft chemical route at 40 °C and pH 6 using H_2O_2 as oxidant have shown excellent UV-shielding properties and decreased catalytic oxidation activity [23–25]. In these studies, the incorporation of Zn into CeO_2 lattice is influenced by H_2O_2. We have reported earlier that the presence of small amount of CeO_2 (10 wt.%) in ZnO lattice enhances hydrogen transfer activity of CeO_2–ZnO materials for cyclohexanone using 2-propanol as hydrogen donor [26]. These studies show that the formation of $Ce_{1-x}Zn_xO_{2-x}$ solid solutions and their catalytic activity are strongly influenced by method preparation [23–26]. In continuation of our work, we report here the detailed characterization of CeO_2–ZnO samples in the whole composition range and discuss their catalytic activity for both cyclohexanol transformation and hydrogen transfer reactions. The pure components and mixed oxides with different compositions were prepared by amorphous citrate process. The composite oxides are found to have better physicochemical properties and catalytic activities compared to individual oxide components. A good correlation has been observed between surface properties and catalytic activity of the composite oxide catalysts for cyclohexanol dehydrogenation and hydrogen transfer reactions. The catalytic studies clearly demonstrate the ability of ceria in promoting organic reactions on acid–base sites.

2. Experimental

2.1. Catalyst preparation

$Ce(NO_3)_3{\cdot}6H_2O$ (CDH Chemicals, India, 99.9%), $Zn(NO_3)_2{\cdot}6H_2O$ and citric acid monohydrate (S.D. Fine Chemicals, India, 99.9%) were used to prepare CeO_2(x mol%)–ZnO mixed oxides. A solid mixture of cerium and zinc nitrates of desired molar ratio was mixed with an equimolar amount of citric acid and heated at 60 °C to form uniform melt which was evacuated to obtain an expanded spongy solid material. This material is transferred to hot air oven at 160 °C for 2 h to obtain amorphous citrate precursor. The calcination of citrate precursor at 550 °C for 3 h produced fine powder of CeO_2–ZnO mixed oxide. Pure ZnO and CeO_2(10%)–ZnO were also prepared from the decomposition of corresponding acetate salts. For preparing CeO_2(10%)–ZnO composite, zinc acetate and cerium acetate salts were dissolved in minimum amount of water to form a thick paste which was dried and calcined at 500 °C in air for 3 h. The ZnO and CeO_2(10%)–ZnO catalysts prepared by this method are designated in the text as ZnO-dec and CeO_2(10%)–ZnO-dec.

2.2. Catalyst characterization

All samples were analysed by X-ray diffraction employing Shimadzu XD-D1 diffractometer using Cu Kα radiation (λ = 1.5418 Å). The UV–vis spectroscopic studies were carried out in diffuse reflectance mode. UV–vis–NIR spectra were recorded on a Varian Cary 5E spectrometer equipped with an integrating sphere coated with polytetrafluoroethylene (PTFE) in the spectral range of 200–2500 nm. The powder samples were made into self-supported pellets of 13 mm diameter and 2 mm thick for measurements. Thermogravimetry analysis of the samples were preformed on Perkin-Elmer TGA-7 apparatus in air (30 ml/min) with linear heating rate (20 °C/min) from room temperature to 800 °C. The CHN analysis of the amorphous citrate precursor was carried out on a Heraeus-CHN-rapid analyzer. Scanning electron microscopy pictures were taken using JEOL JSM-5300 microscope (acceleration voltage 15 kV). The sample powders were deposited on a carbon tape before mounting on a sample holder. The surface acidity and basicity of the composite oxide catalysts were determined by employing titration method [27]. Prior to the acid–base measurement, the catalyst samples were calcined at 500 °C in high pure nitrogen and cooled to room temperature. The standard solutions of *n*-butylamine and trichloroacetic acid were prepared in double distilled dry benzene. 0.5 g of oxide catalyst was kept for equilibration separately with 0.025 M of *n*-butylamine and trichloroacetic acid solutions for 24 h. The acid–base property of the catalysts was evaluated by mutual titration employing neutral red as indicator. The acidity and basicity of catalyst samples were obtained in mmol g^{-1} from the respective equivalent volumes of *n*-butylamine and trichloroacetic acid consumed.

2.3. Catalytic activity studies

The vapour phase cyclohexanol dehydrogenation and hydrogen transfer reactions of cyclohexanone with 2-propanol were carried out using 0.4–1.0 g catalyst packed in a fixed bed flow glass reactor. The reaction temperature was continuously monitored by a thermocouple placed in the middle of the catalyst bed. Prior to the reaction, the catalysts were activated in oxygen flow (25 ml/min) for 3 h at 450 °C and brought to the reaction temperature. The reactants were fed through the top of the reactor by means of a motor driven infusion pump (SP2S-MC model, Electronic Corporation, India). Pure nitrogen was used as a carrier gas at a flow rate of 30 ml/min. The liquid products were collected in an ice trap and analyzed by gas chromatograph (AIMIL-Nucon 5765, India) using flame ionization detector and 20% carbowax column. The column temperature was controlled from 70 to 190 °C at a linear heating rate of 10 °C/min. Each reaction run continued for 1 h and at the end of the each run catalysts were reactivated at 450 °C in oxygen for 3 h for a subsequent run.

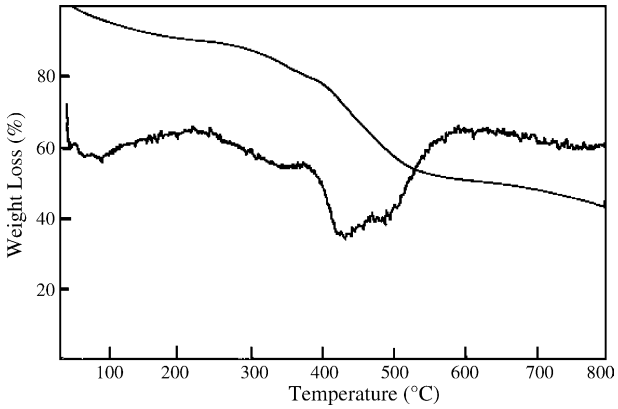

Fig. 1. TGA profile of the amorphous citrate precursor for CeO_2 (40%)–ZnO catalyst.

3. Results and discussion

3.1. Characterization of amorphous citrate precursor

The CeO_2, ZnO and CeO_2–ZnO mixed phases containing 10, 20, 40, 60 and 80 mol% of CeO_2 were prepared by amorphous citrate process. In this process, the mixed metal oxide precursor is an amorphous solid containing all required metal ions mixed intimately with an organic polyfunctional acid. The citrate process has been proved to be an effective method for the preparation of well dispersed composite oxides and solid solutions [16,28,29]. Fig. 1 shows the TGA curve of a typical amorphous precursor of CeO_2(40%)–ZnO material in air atmosphere. In TG analysis, the decomposition of citrate precursor to corresponding mixed oxides occurs in a wide temperature range with major weight loss observed between 350 and 550 °C. The total weight loss in TG analysis is ~44.6% which corresponds to the loss of one molecule of citric acid for each Ce^{3+} or Zn^{2+} ions. All the mixed oxide materials show similar weight loss behavior in TG analysis. During the preparation of composite oxides by amorphous citrate process, it is reported that all citric acid molecules are retained and distributed evenly in the amorphous precursor [28]. This is verified further by CHN analysis performed on amorphous precursor samples selected from three different locations of the expanded solid. The CHN data in Table 1 shows good homogeneity of CeO_2(40%)–ZnO amorphous precursor before calcination at 550 °C. The percentage values of C, H and N of all precursor samples are similar within the experimental error. In amorphous citrate process water of crystallization of individual salts is removed rapidly from the molten mixture at 60 °C in vacuum. Subsequent heat treatment at 160 °C results in the decomposition of nitrate ions as evident from the low nitrogen content of the precursor (Table 1). Assuming that the precursor at this stage contains Ce^{3+} and Zn^{2+} ions along with citric acid, the carbon and hydrogen content of CeO_2(40%)–ZnO precursor is calculated to be 25.6 and 2.8%, respectively. These values are in good agreement with the experimental values presented in Table 1. The CHN data suggests that in the microscopic scale the amorphous precursor is well dispersed with no local agglomeration and contains one molecule of citric acid for each Ce^{3+} or Zn^{2+} ions.

Table 1
CHN analysis of the CeO_2(40%)–ZnO amorphous citrate precursor samples selected from three different locations of the expanded solid

	Amorphous precursor (CeO_2(40%)–ZnO)		
	Sample 1	Sample 2	Sample 3
%C	24.50	25.20	24.80
%H	02.90	02.90	03.00
%N	01.55	01.60	01.70

3.2. Characterization of CeO_2–ZnO composite oxide catalysts

3.2.1. XRD patterns

The X-ray diffraction patterns of CeO_2, ZnO and CeO_2–ZnO mixed oxide phases are shown in Fig. 2. The XRD peaks for pure ceria are observed at $2\theta = 28.8$, 33.4, 47.7 and 56.7 corresponding to (1 1 1), (2 0 0), (2 2 0) and (3 1 1) planes, respectively. The diffraction peaks are characteristic of cubic ceria phase with fluorite structure (JCPDS card number 34-394). Similarly XRD peaks for ZnO are observed at $2\theta = 32.0$, 34.6, 36.5, 47.7 and 56.8 corresponding to (1 0 0), (0 0 2), (1 0 1), (1 0 2) and (1 1 0) planes, respectively. The diffraction patterns indicate that pure CeO_2 and ZnO samples are more crystalline compared to

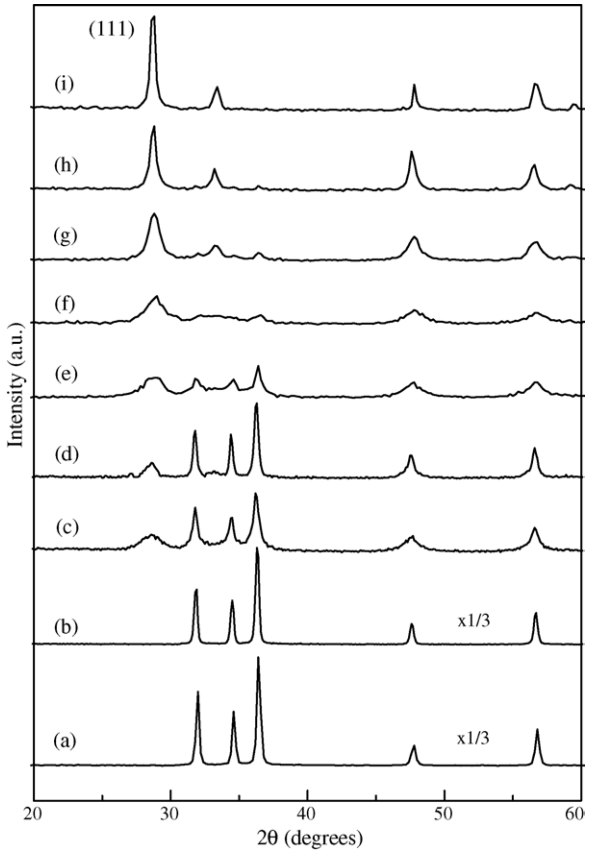

Fig. 2. X-ray diffraction patterns for (a) ZnO; (b) ZnO-dec; (c) CeO_2(10%)–ZnO; (d) CeO_2(10%)–ZnO-dec; (e) CeO_2(20%)–ZnO; (f) CeO_2(40%)–ZnO; (g) CeO_2(60%)–ZnO; (h) CeO_2(80%)–ZnO and (i) CeO_2.

CeO_2–ZnO mixed phase materials. The XRD profile of ZnO has been affected significantly by the addition of 10% CeO_2 in both the preparative methods (Fig. 2(c and d)). The diffraction patterns also show the formation of mixed oxide materials containing well-dispersed phases of semi-crystalline nature from both the constituent oxides. When ceria content is increased from 20 to 80 mol% in the mixed oxide, the intensity of ZnO reflections at (1 0 0), (0 0 2) and (1 0 1) decreased quite rapidly while that of the CeO_2 (1 1 1) peak is increased. This is due to the higher scattering factor of Ce^{4+} ions compared to Zn^{2+} ions in the CeO_2–ZnO composite oxide catalysts. The scattering factor f of an atom depends on $\sin\theta/\lambda$ (θ = scattering angle and λ = wavelength of X-ray) and atomic number Z. Hence in a crystal structure, it is difficult to detect lighter atoms in presence of heavier atoms due to weak diffraction of the former.

It is observed in Fig. 2 that the individual peak positions of CeO_2 and ZnO remain unaltered in the composite oxides. This is an indication that the composite oxides contain individual phases of ceria and ZnO although the dissolution of small amount of ZnO in ceria and vice versa cannot be ruled out completely. Fluorite type substitutional solid solutions are known for systems like CeO_2–ZrO_2, CeO_2–Mn_2O_3, CeO_2–CuO due to the structural similarities of the constituents [12,30,31]. However, the present study on ZnO–CeO_2 system does not show clear evidence of the formation of solid solution. If Ce^{4+} ions in the fluorite lattice were to be substituted by Zn^{2+} ions, there should be a change in the 2θ values of the diffraction peaks in Fig. 2 affecting the lattice constant which is normally observed in the substitutional solid solutions like CeO_2–ZrO_2 [12]. The insertion of smaller cations such as Mg^{2+} (0.72 Å), which is comparable to that of Zn^{2+} (0.68 Å), into the interstitial positions of CeO_2 lattice forming a non-equilibrium solid solution has been reported in the case of CeO_2–MgO system [16]. However, the formation of such a substitutional solid solution is of limited nature and may not occur in the entire composition range. In the present case, the formation of composition limited solid solution is elusive due to the method of preparation. The formation of $Ce_{1-x}Zn_xO_{2-x}$ (x = 0–0.56) solid solutions have been reported using H_2O_2 as oxidant in the reaction mixture where oxidation of Ce(III) to Ce(IV) occurs [23–25]. In this work the amorphous citrate precursor is a polymerized citric acid matrix acting as a dispersing agent for Ce^{3+} and Zn^{2+} ions. Upon calcination, mostly the formation of individual oxide phases are favoured. There is a possibility of forming interstitial $Zn_xCe_{1-2x}{}^{4+}Ce_{2x}{}^{3+}O_2$ solid solutions at the grain boundary region due to the diffusion of some amount Zn^{2+} ions into ceria lattice.

The CeO_2 (1 1 1) peak at $2\theta = 28.8^\circ$ has been used for X-ray line broadening analysis to calculate the crystallite size of ceria by Scherrer's equation. The data summarized in Table 2 show that the particle size of ceria is not affected up to 40 mol% of ceria content in CeO_2–ZnO composite oxide. The ceria particles are well dispersed with an average particle size of ~5 nm. However, the particle size increases beyond 40% of ceria reaching maximum of ~22 nm for pure ceria crystallites. In summary the CeO_2–ZnO composite oxides prepared by amorphous citrate process contain well dispersed nanosize ceria particles.

3.2.2. UV–vis diffuse reflectance study

The UV–vis-diffuse reflectance spectra of CeO_2–ZnO mixed oxides along with pure CeO_2 and ZnO phases are presented in Figs. 3 and 4. Pure ZnO shows a broad absorption feature in Fig. 3(a) with an absorption edge around 400 nm. This absorption feature is the characteristic of semiconducting ZnO particles with a band gap of ~3.4 eV [32]. Pure CeO_2 prepared by amorphous citrate process shows two intense bands along with a broad absorption feature in the UV-region of the spectrum in Fig. 3(f). Crystalline cerium dioxide has a band gap of 3.1 eV and absorbs strongly in the UV region with the absorption threshold near 400 nm. The distinct absorption bands at 256 and 296 nm are assigned to $O^{2-} \rightarrow Ce^{3+}$ and $O^{2-} \rightarrow Ce^{4+}$ charge transfer transitions [33]. Addition of ceria to ZnO changes the absorption features showing new narrow bands at 230, 250–265, 280–295 and 330–345 nm in the UV region of the spectra due to localized transitions (Fig. 3(b–e)). Such narrow bands have been observed earlier for ultrafine ceria particles dispersed in silica and alumina matrices [34,35]. The nano-size ceria particles are reported to show localized $O \rightarrow Ce$ charge transfer transitions involving a number of surface Ce^{4+} ions with variety of coordination numbers [33–35]. The coordination number of surface Ce^{4+} ions can vary between 4 and 8, the later being the coordination number of bulk Ce^{4+} in the fluorite structure [34]. The narrow absorption bands in the UV region observed in the case of CeO_2–ZnO catalysts indicate that CeO_2 component is dispersed in the form of nano-size crystallites in the composite oxide. In the visible region of the spectrum in Fig. 4, the CeO_2 containing composite oxides show two broad bands of very low intensity between

Table 2
Physicochemical characteristics of CeO_2–ZnO oxide catalysts tested for cyclohexanol dehydrogenation activity at 350 °C

Sample	Crystallite size (Å)[a]	Surface area ($m^2\ g^{-1}$)	Conversion (mol%)	Selectivity (%)	
				Cyclohexanone	Cyclohexene
ZnO	–	23.4	13.2	96.6	3.4
CeO_2(20%)–ZnO	51	40.0	25.8	92.0	8.0
CeO_2(40%)–ZnO	53	35.7	29.9	90.2	9.8
CeO_2(60%)–ZnO	99	32.1	18.6	87.8	12.2
CeO_2(80%)–ZnO	184	30.6	13.3	85.6	14.4
CeO_2	218	34.2	5.3	70.5	29.5

[a] For ceria phase.

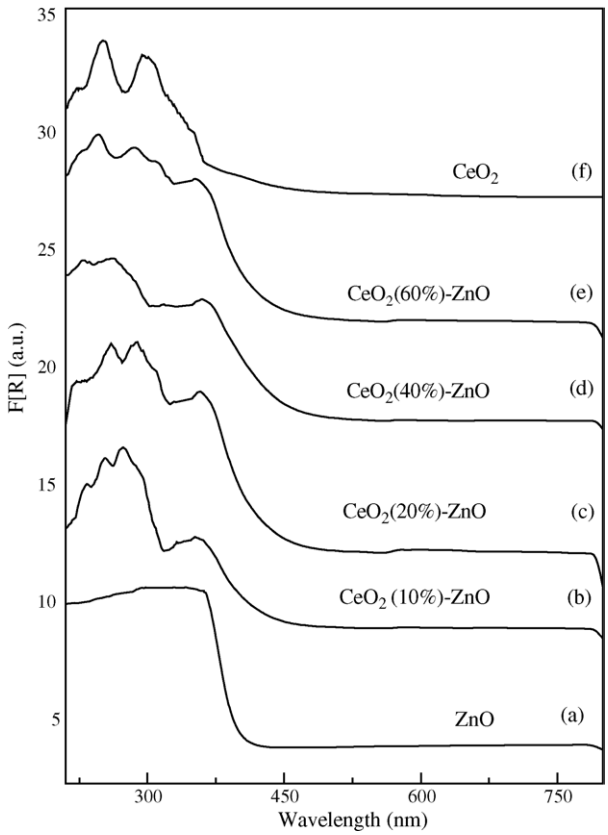

Fig. 3. The UV–vis–DRS spectra of catalysts prepared by amorphous citrate process (a) ZnO; (b) CeO_2(10%)–ZnO; (c) CeO_2(20%)–ZnO; (d) CeO_2(40%)–ZnO; (e) CeO_2(60%)–ZnO and (f) CeO_2.

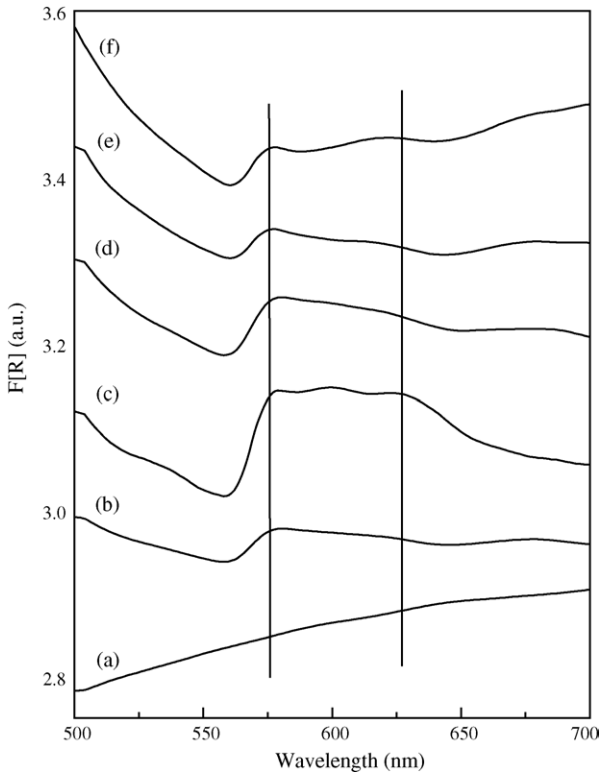

Fig. 4. The UV–vis–DRS spectra of catalysts prepared by amorphous citrate process (a) ZnO; (b) CeO_2(10%)–ZnO; (c) CeO_2(20%)–ZnO; (d) CeO_2(40%)–ZnO; (e) CeO_2(60%)–ZnO and (f) CeO_2.

550 and 650 nm. The twin absorption features observed at 580 and 620 nm for CeO_2–ZnO composite oxides are completely absent for ZnO particles. These absorption features are attributed to reduced CeO_2 sites on the surface ($Ce^{3+} \rightarrow Ce^{4+}$) of the crystallites [36]. The UV–vis-diffuse reflectance study demonstrates the availability of low coordinated surface Ce^{4+} and Ce^{3+} ions in CeO_2–ZnO composite oxides produced by citrate method.

3.2.3. Near IR study

The near IR spectra of CeO_2–ZnO mixed oxides in the range of 1200–2500 nm are shown in Fig. 5. The near infrared portion of the diffuse reflectance spectrum covers the overtones and combination bands of the fundamental stretching frequencies of surface molecular groups such as H_2O and –OH [37]. The overtone and combination bands are smaller in intensity and excellently measured in diffuse reflectance mode than in transmission mode because of large scattering involved in the NIR region. The NIR–DRS spectra shown in Fig. 5 indicate the presence of water and hydroxyl groups in CeO_2–ZnO composite materials. The three prominent bands observed at 1440, 1935 and 2215 nm in the DR–NIR spectra of CeO_2–ZnO samples are attributed to the first overtone of hydroxyl groups ($2\nu_{O-H}$), combination band corresponding to hydroxyl stretching and bending ($\nu_{OH} + \delta_{H_2O}$) and combination band of ($\nu_{OH} + \delta_{surface\,OH}$) vibrational modes, respectively. Among all the spectra in Fig. 5, pure cerium dioxide shows intense NIR peaks while CeO_2–ZnO mixed oxides have lesser intense peaks in this region. The intensity of the peaks in NIR region depends strongly on water and surface hydroxyl content [37]. In case of pure ceria, the intense NIR bands observed are the overtone and combination bands traced to the surface hydroxyl groups present on ceria particles with IR bands at 3772 and 3668 cm^{-1} [36].

3.2.4. SEM study

The scanning electron micrographs of CeO_2, ZnO and CeO_2–ZnO mixed oxides are presented in Fig. 6. The SEM pictures of ZnO powder shows polycrystalline agglomerated particles (Fig. 6(a)). Pure CeO_2 shows particles of uniform size and shape compared to pure ZnO (Fig. 6(b)). Addition of ceria to ZnO seems to influence the morphology and size of composite oxide particles. The citrate process leads to the formation of homogeneous particles of regular shape (Fig. 6(c)). The SEM pictures in Fig. 6(c and d) indicate different textures for CeO_2–ZnO catalysts prepared by citrate process and decomposition of acetate salts. In citrate process, the amorphous precursors are prepared by rapid evacuation of the molten mixture of corresponding salts and citric acid. Considerable swelling of the citrate precursor takes place in the presence of cerium salts contributing to the mutual dispersion of oxide components. This citrate process enhances the surface area (Table 2) and uniform textural properties in CeO_2–ZnO materials compared to acetate precursor route.

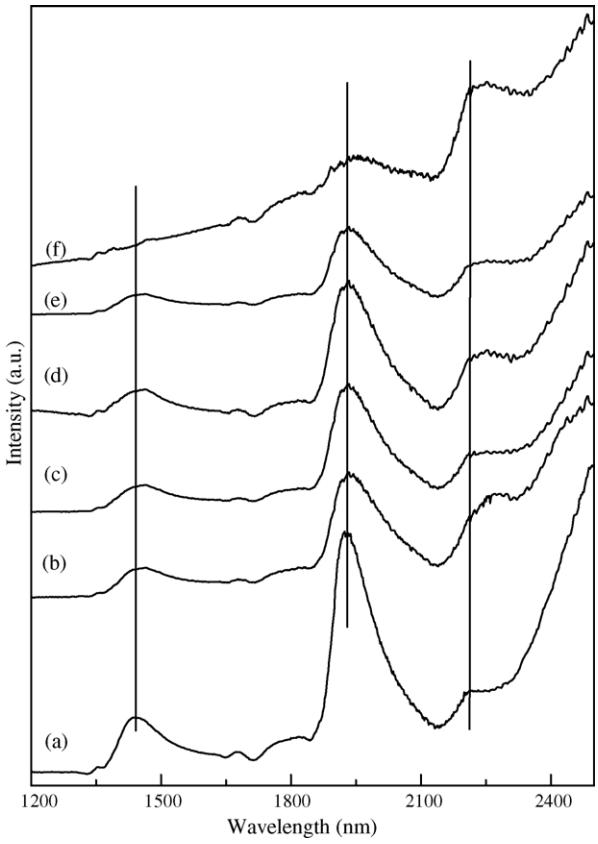

Fig. 5. NIR-diffuse reflectance spectra of catalysts prepared by amorphous citrate process (a) CeO_2; (b) CeO_2(80%)–ZnO; (c) CeO_2(60%)–ZnO; (d) CeO_2(40%)–ZnO; (e) CeO_2(20%)–ZnO and (f) ZnO.

3.3. Catalytic reaction studies

3.3.1. Cyclohexanol transformation

Cyclohexanol transformation reaction was carried out over CeO_2–ZnO catalysts in vapour phase in the temperature range 325–375 °C. Table 2 summarizes the catalytic activity data for various CeO_2–ZnO catalysts after 1 h of the reaction at 350 °C and WHSV of 19.0 h^{-1}. Pure ZnO catalyst shows 13.2 mol% conversion and 96.6% selectivity to cyclohexanone. Addition of CeO_2 to ZnO enhances the activity and conversion reaches maximum value at 40% CeO_2 content. However, there is a marginal decrease in selectivity to cyclohexanone compared to pure ZnO. The ZnO rich phases show better catalytic activity compared to ceria rich phases. Pure ceria shows minimum catalytic activity and selectivity for cyclohexanone. It is therefore suggestive that smaller amounts of CeO_2 up to 40 mol% can be added as promoter for cyclohexanol dehydrogenation using ZnO catalysts.

The cyclohexanol transformation reaction has been studied on transition, alkali and alkaline earth metal oxides and supported bimetallic catalysts to evaluate the surface acid–base and catalytic properties of these materials [21,38–40]. The oxide catalysts show stable catalytic activity for this reaction compared to the metallic catalysts and selectivity depends on the acid–base property of oxide surface. It is observed that dehydration of cyclohexanol to cyclohexene occurs on surface Brønsted acid sites while dehydrogenation to cyclohexanone is facilitated by basic sites originating from lattice oxygen ions [38]. Table 3 shows the acid–base property of the composite oxides along with that of pure oxides. It is seen that CeO_2 contains nearly equal distribution of both acidic and basic sites while ZnO exposes 90% of strong basic sites on the surface. ZnO is a known solid base with some acidic nature while CeO_2 seems to exhibit weak basic and acidic properties [18,41]. In the case of CeO_2–ZnO composite oxides, the number of basic sites is found to increase up to 40% CeO_2 and then there is a gradual decrease with further increase in CeO_2 content. However, the density of the basic sites in CeO_2–ZnO composite remains same up to 40 mol% of ceria and decreases further with increased ceria content. However, the acidity of the composite oxide increases linearly with addition of ceria content. The number of acidic sites per unit surface area is directly related to the percentage of ceria present in the composite oxide. Sato and co-workers reported similar reactivity trend for phenol alkylation on CeO_2–MgO catalysts where alkylation activity has been correlated with number of basic sites on the catalyst [16]. The presence of ceria in the CeO_2–MgO catalyst is found to increase the total number of weak basic sites. In this study, the presence of Ce^{4+} ions in ZnO matrix can modify the physicochemical properties of composite oxide catalyst exposing low coordinated Ce^{4+} and Zn^{2+} ions which can function as Lewis acid sites at the surface. The UV–DRS study provides evidence for existence of such low coordinated cerium ions on the surface of these particles. The charge/radius ratio for Ce^{4+} is 4.26 C $Å^{-1}$ which is greater than the value of 2.70 C $Å^{-1}$ observed for Zn^{2+}. Due to higher charge to radius ratio, Ce^{4+} ions are expected to be more Lewis acidic compared to Zn^{2+} ions under identical conditions. Accordingly, CeO_2 will have more acidic sites compared to ZnO. The ZnO, on the other

Table 3
Activity of CeO_2–ZnO composite oxide catalysts for cyclohexanol dehydrogenation reaction

Catalyst	Basic sites (mmol g^{-1})	Acid sites (mmol g^{-1})	Basic sites (μmol m^{-2})	Acid sites (μmol m^{-2})	Reaction rate		Turnover frequency (h^{-1})[a]
					Mmol h^{-1} m^{-2}	Mmol h^{-1} g^{-1}	
ZnO	0.35	0.03	14.2	1.0	0.42	24.5	28
CeO_2(20%)–ZnO	0.45	0.10	11.2	2.5	0.48	48.0	44
CeO_2(40%)–ZnO	0.49	0.13	13.7	3.6	0.63	56.2	56
CeO_2(60%)–ZnO	0.32	0.14	9.9	4.3	0.43	34.5	45
CeO_2(80%)–ZnO	0.22	0.16	7.1	5.2	0.32	24.4	39
CeO_2	0.17	0.19	4.9	5.5	0.11	9.4	21

[a] On basic sites.

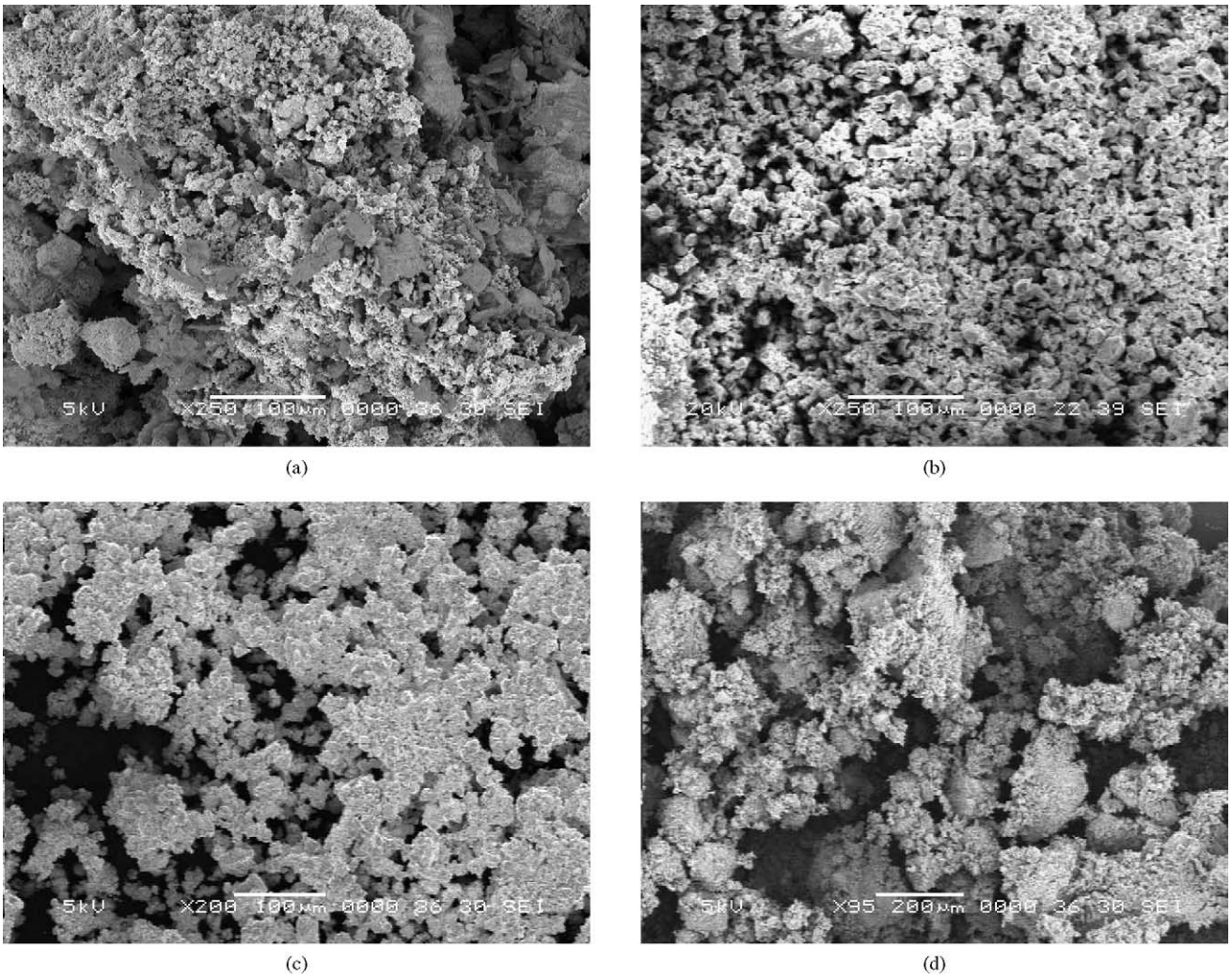

Fig. 6. Scanning electron micrographs of (a) ZnO; (b) CeO_2; (c) CeO_2(40%)–ZnO; (d) CeO_2(10%)–ZnO-dec (a, b and c are prepared by amorphous citrate process).

hand, is more ionic and contains stronger basic sites compared to ceria. Therefore, CeO_2–ZnO composite oxide is likely to have more acidic sites compared to pure ZnO which is reported here.

The increase in the total number of basic sites per gram of the composite catalysts at lower CeO_2 content is attributable to Lewis basic sites present as low coordinated O^{2-} ions. However, it is noted from Table 2 that the density of the basic sites remains same up to 40 mol% of ceria. This is due to the fact that the change in basic property of the composite oxide is not due to the modification of oxide lattices rather it is due to external factors such as exposure of low coordinated O^{2-} ions on surface and formation of small crystallites, predominantly related to the method of preparation. Ceria and ceria added ZnO composite oxides prepared by amorphous citrate process also show improved surface area when compared to ZnO (Table 2). A good correlation is seen in Tables 2 and 3 between the surface properties and catalytic activity of CeO_2–ZnO catalysts. Table 3 shows the rate of the reaction and turnover frequency for the CeO_2–ZnO catalysts. The reaction data shows that presence of ceria in the ZnO matrix clearly promotes the catalytic activity up to 40 mol%. However, the rate of reaction and turnover frequency are found to be low for ceria rich phases. Fig. 7 shows the effect of reaction time on catalytic activity of CeO_2, ZnO and CeO_2–ZnO composite oxide catalysts studied for 5 h at 375 °C. The oxide catalysts containing CeO_2 as a major phase show a marginal decrease of about 3% in the conversion activity at the end of the fifth hour of the study. The time on stream study shows slow deactivation pattern through the entire period investigated and the deactivation being faster in the first part of the reaction. For example the TOF is found to decrease from 21 to 18 after 5 h of reaction on CeO_2 catalyst.

3.3.2. Hydrogen transfer reaction of cyclohexanone with 2-propanol

The catalytic activity of ZnO and CeO_2(10%)–ZnO catalysts prepared by both amorphous citrate process and decomposition of acetate precursor have been tested for vapour phase hydrogen transfer reaction of cyclohexanone using 2-propanol as hydrogen donor at 275 °C. Cyclohexanol is the only product observed in this reaction with selectivity greater than 98%. There is no appreciable conversion of pure cyclohexanol on the catalyst surface under identical reaction conditions. This

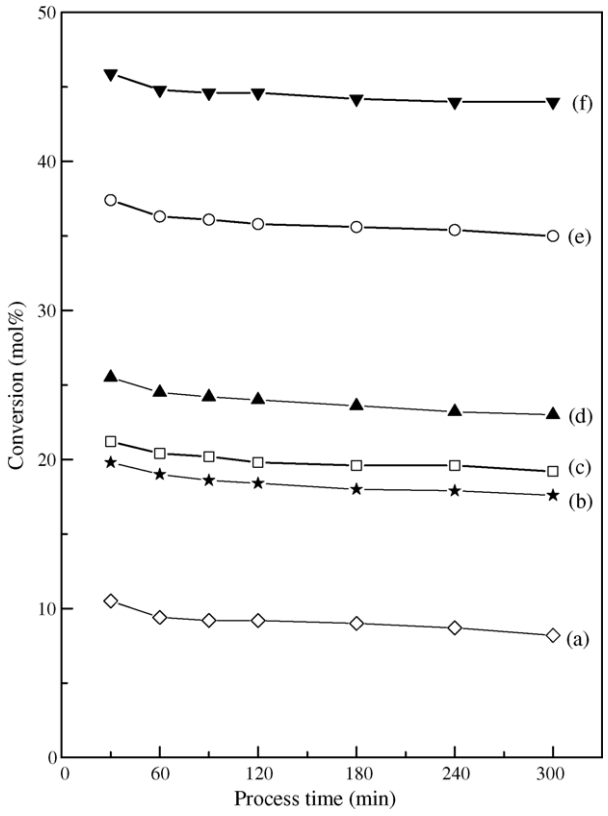

Fig. 7. Cyclohexanol conversion with process time over catalysts prepared by amorphous citrate process studied for 5 h at 375 °C and WHSV of 19.0 h^{-1}, (a) CeO_2; (b) CeO_2(80%)–ZnO; (c) ZnO; (d) CeO_2(60%)–ZnO; (e) CeO_2(20%)–ZnO and (f) CeO_2(40%)–ZnO.

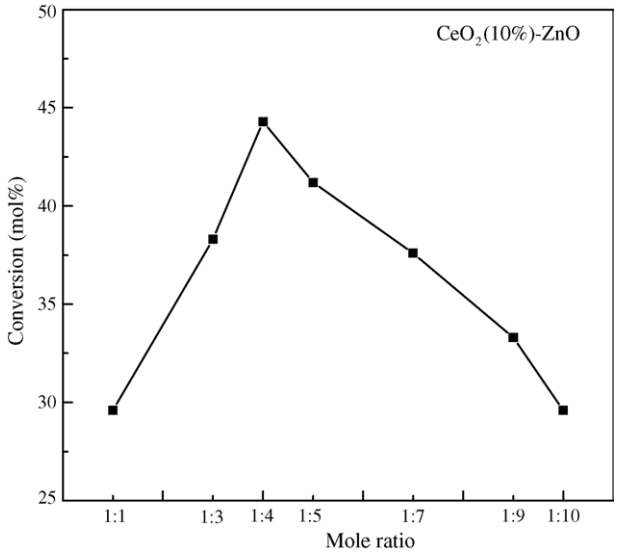

Fig. 8. Effect of mole ratio (cyclohexanone:2-propanol) on the hydrogen transfer activity at 275 °C on CeO_2(10%)–ZnO catalyst prepared by amorphous citrate process.

excludes the possibility of further reaction of cyclohexanol via dehydrogenation or dehydration steps. However, there is a possibility that cyclohexanone can react further on the catalyst surface producing condensation products such as cyclohexyldencyclohexanone. These products being strongly adsorbed on the catalyst surface, may not be detected in the reaction mixture. This may also partially responsible for deactivation of the catalysts as described later in this section. Fig. 8 shows the effect of mole ratio of the reactants on the catalytic activity of CeO_2(10%)–ZnO catalyst. The catalytic activity peaks at cyclohexanone to 2-propanol molar ratio of 1:4. Similar trend has also been observed for all catalyst samples. This observation indicates that both the reactant species are simultaneously adsorbed on the surface during the reaction. Such a phenomenon where both the reactants are simultaneously co-adsorbed on the surface during the reaction is governed by the Langmuir–Hinshelwood type surface reaction mechanism which has been reported earlier for hydrogen transfer reactions [42]. Hydrogen transfer reactions have been studied on variety of catalyst materials under homogeneous and heterogeneous conditions. Vapour-phase transfer hydrogenation is reported on ZrO_2, MgO/B_2O_3 [43], $Zr_{0.8}(M)_{0.2}O_2$ (M = Fe, Co, Ni, Cu, Cr and Mn) [44], CeO_2–ZrO_2 [23] and hydrous zirconia [42]. These oxide systems show basic or amphoteric characters. The reaction mechanism is similar to the Meerwein–Ponndorf–Verley type reduction and proceeds in a concerted manner on an oxide surface. The hydrogen accepter and donor are adsorbed on adjacent acidic and basic sites facilitating hydrogen transfer reaction. The transfer of hydride ion from donor to acceptor has been found to be the rate-limiting step for such reactions [42].

Table 4 shows the surface area, acid–base properties and catalytic activity in terms of average conversion for 1 h of reaction at 275 °C for ZnO and CeO_2(10%)–ZnO catalysts prepared by both citrate process and acetate precursor decomposition. The preparative method is found to be crucial for physicochemical characteristics of final catalysts. In citrate process, addition of ceria to ZnO increases the surface area. The composite catalysts show a considerable increase in acidity and a moderate increase in the basicity. Addition of smaller amounts of ceria to ZnO,

Table 4
Hydrogen transfer activity of CeO_2–ZnO catalysts at 275 °C and WHSV = 9.9 h^{-1}

Catalyst[a]	Surface area ($m^2\ g^{-1}$)	Acidity (mmol g^{-1})	Basicity (mmol g^{-1})	Acidity (μmol m^{-2})	Basicity (μmol m^{-2})	Conversion (mol%)	Reaction rate	
							Mmol $h^{-1}\ m^{-2}$	Mmol $h^{-1}\ g^{-1}$
Entry 1	10.2	0.03	0.19	0.0029	0.0156	9.7	0.48	9.7
Entry 2	23.4	0.04	0.35	0.0025	0.0149	16.8	0.36	16.8
Entry 3	18.5	0.08	0.26	0.0043	0.0140	24.3	0.67	24.8
Entry 4	42.1	0.12	0.43	0.0028	0.0102	44.3	0.55	46.3

[a] Entry 1 = ZnO-dec; entry 2 = ZnO; entry 3 = CeO_2(10%)–ZnO-dec and entry 4 = CeO_2(10%)–ZnO. Entries 2 and 4 are prepared by amorphous citrate process.

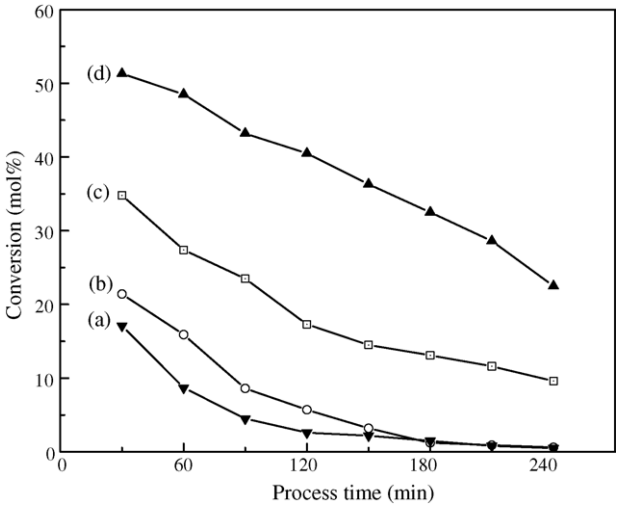

Fig. 9. Effect of process time on the catalytic activity of (a) ZnO-dec; (b) ZnO; (c) CeO_2(10%)–ZnO-dec and (d) CeO_2(10%)–ZnO (b and c are prepared by amorphous citrate process).

irrespective of preparative method employed, shows significant increase on the hydrogen transfer activity. The key factor for the enhancement of acid–base properties of the composite oxides is the dispersion of ceria as nanosize crystallites over the ZnO surface. The reaction rate observed per unit surface area of the material clearly indicates that the presence of ceria in ZnO lattice promotes hydrogen transfer reaction. Fig. 9 shows conversion versus process time plots for CeO_2–ZnO catalysts at 300 °C and WHSV of 9.9 h^{-1}. All catalysts deactivate gradually with process time. Pure ZnO deactivates rapidly with total loss of catalytic activity after two hours of the reaction. The ZnO catalyst prepared by citrate method shows slightly higher initial activity compared to ZnO-dec but both samples get deactivated at about same process time. However, the behavior of CeO_2(10%)–ZnO and CeO_2(10%)–ZnO-dec catalysts with time on stream is interesting. They show higher conversions and the rate of deactivation is lesser compared to that of pure ZnO materials prepared by both methods. As observed from acid–base data in Table 4, the CeO_2(10%)–ZnO catalyst shows higher catalytic activity and less prone to deactivation with time on stream compared to ZnO catalyst.

4. Conclusions

The citrate process is particularly effective for the preparation of nanosize CeO_2–ZnO mixed oxides of uniform composition. The amorphous precursor prepared during the citrate process is a homogeneous solid and contains one molecule of citric acid per Ce^{4+} or Zn^{2+} ions as identified from the CHN analysis in microscopic scale. The CeO_2–ZnO mixed oxides contain individual phases of ceria and zinc oxide in finely dispersed form. UV–vis–DRS study indicates the presence of low coordinate surface sites and defect centres on these mixed oxides. There is evidence from NIR study for the presence of structural hydroxyl groups on the surface of composite oxide, mainly on ceria. The acid–base properties of ZnO matrix are influenced by ceria content. New acidic sites are generated in mixed oxides along with increased number of basic sites which correlates well with catalytic activities observed for both cyclohexanol dehydrogenation and hydrogen transfer reactions. This study demonstrates the promoting effect of ceria for cyclohexanol dehydrogenation and hydrogen transfer reactions over CeO_2–ZnO mixed phases prepared by amorphous citrate process. Hydrogen transfer activity is found to be higher on CeO_2(10%)–ZnO catalyst prepared by citrate method.

Acknowledgments

Financial grants from CSIR (No. 01(1516)/98/EMR-II) and DRDO (No. ERIP/ER/0300231/M/01), New Delhi, are gratefully acknowledged. We thank colleagues at NIOT for extending some experimental facilities.

References

[1] A. Trovarelli, Catal. Rev.—Sci. Eng. 38 (1996) 439.
[2] A. Trovarelli, C. Leitenburg, M. Boaro, G. Dolcetti, Catal. Today 50 (1999) 353.
[3] S. Imamura, Y. Okumura, T. Nishio, K. Utani, Y. Matsumura, Ind. Eng. Chem. Res. 37 (1998) 1136.
[4] G. Neri, A. Pistone, C. Milone, S. Galvagno, Appl. Catal. B: Environ. 38 (2002) 321.
[5] M. Dokiya, Solid State Ionics 152–153 (2002) 383.
[6] L. Pino, A. Vita, M. Cordaro, V. Recupero, M.S. Hegde, Appl. Catal. A: Gen. 243 (2003) 135.
[7] D. Srinivas, C.V.V. Satyanarayana, H.S. Potdar, P. Ratnasamy, Appl. Catal. A: Gen. 246 (2003) 323.
[8] A. Martinez-Arias, M. Fernandez-Gracia, O. Galvez, J.M. Coronado, J.A. Anderson, J.C. Conesa, J. Soria, G. Munuera, J. Catal. 195 (2000) 207.
[9] W. Liu, M. Flytzani-Stephanopoulos, J. Catal. 153 (1995) 304.
[10] C. Leitenburg, A. Trovarelli, J. Kašpar, J. Catal. 166 (1997) 98.
[11] P. Fornasiero, R. Di Monte, G. Ranga Rao, J. Kašpar, S. Meriani, A. Trovarelli, M. Graziani, J. Catal. 151 (1995) 168.
[12] G. Ranga Rao, P. Fornasiero, R. Di Monte, J. Kašpar, G. Vlaic, G. Balducci, S. Meriani, G. Gubitosa, A. Cremona, M. Graziani, J. Catal. 162 (1996) 1.
[13] P. Fornasiero, G. Ranga Rao, J. Kašpar, F.L. Erario, M. Graziani, J. Catal. 175 (1998) 269.
[14] G. Ranga Rao, H.R. Sahu, B.G. Mishra, Colloid Surf. A: Physicochem. Eng. Asp. 220 (2003) 261.
[15] S. Sato, K. Koizumi, F. Nozaki, Appl. Catal. A: Gen. 133 (1995) 7.
[16] S. Sato, K. Koizumi, F. Nozaki, J. Catal. 178 (1998) 264.
[17] P. Käβner, M. Baerns, Appl. Catal. A: Gen. 139 (1996) 107.
[18] A. Auroux, P. Artizzu, I. Monaci, E. Rombi, V. Solinas, G. Petrini, J. Chem. Soc., Faraday Trans. 92 (1996) 2619.
[19] M.A. Cutrufello, I. Ferino, V. Solinas, A. Primavera, A. Trovarelli, A. Auroux, C. Picciau, Phys. Chem. Chem. Phys. 1 (1999) 3369.
[20] M.I. Zaki, M.A. Hasan, L. Pasupulety, Langmuir 17 (2001) 768.
[21] D. Martin, D. Duprez, J. Mol. Catal. A: Chem. 118 (1997) 113.
[22] D. Martin, D. Duprez, J. Phys. Chem. 100 (1996) 9429.
[23] R. Li, S. Yabe, M. Yamashita, S. Momose, S. Yoshida, S. Yin, T. Sato, Solid State Ionics 151 (2002) 235.
[24] R. Li, S. Yabe, M. Yamashita, S. Momose, S. Yoshida, S. Yin, T. Sato, Mater. Chem. Phys. 75 (2002) 39.
[25] S. Yabe, M. Yamashita, S. Momose, K. Tahira, S. Yoshida, R. Li, S. Yin, T. Sato, Inter. J. Inorg. Mater. 3 (2001) 1003.
[26] B.G. Mishra, G. Ranga Rao, B. Poongodi, Proc. Indian Acad. Sci. (Chem. Sci.) 115 (2003) 561.

[27] G. Ranga Rao, H.R. Sahu, B.G. Mishra, React. Kinet. Catal. Lett. 78 (2003) 151.
[28] C. Marcilly, P. Courty, B. Delmon, J. Am. Ceram. Soc. 53 (1970) 56.
[29] N. Ma, Y. Yue, W. Hua, Z. Gao, Appl. Catal. A: Gen. 251 (2003) 39.
[30] M. Machida, M. Uto, M. Kurogi, T. Kijima, J. Mater. Chem. 11 (2001) 900.
[31] J. Xiaoyuan, L. Guanglie, Z. Renxian, M. Jianxin, C. Yu, Z. Xiaoming, Appl. Surf. Sci. 173 (2001) 208.
[32] M.A. Valenzuela, P. Bosch, J. Jimenez-Becerrill, O. Quiroz, A.I. Paez, J. Photochem. Photobiol. A: Chem. 148 (2002) 177.
[33] A. Bensalem, J.C. Muller, F. Bozon-Verduraz, J. Chem. Soc. Faraday Trans. 88 (1992) 153.
[34] A. Bensalem, F. Bozon-Verduraz, M. Delamar, G. Bugli, Appl. Catal. A: Gen. 121 (1995) 81.
[35] M.I. Zaki, G.A.M. Hussein, S.A.A. Mansour, H.M. Ismail, G.A.H. Mekhemer, Colloid Surf. A: Physicochem. Eng. Asp. 127 (1997) 47.
[36] C. Binet, A. Badri, J.-C. Lavalley, J. Phys. Chem. 98 (1994) 6392.
[37] L.M. Coyne, J. Bishop, L. Scattergood, A. Banin, G. Carle, J. Orenberg, Spectroscopic characterization of minerals and their surfaces, in: L.M., Coyne, S.W.S., McKeever, D.F., Blake (Eds.), ACS Symposium Series, Washington, 1990.
[38] C.P. Bezouhanova, M.A. Al-Zihari, Catal. Lett. 11 (1991) 245.
[39] D.V. Cesar, C.A. Peréz, V.M.M. Salim, M. Schmal, Appl. Catal. A: Gen. 176 (1999) 205.
[40] V.Z. Fridman, A.A. Davydov, J. Catal. 195 (2000) 20.
[41] V.R. Choudhary, V.H. Rane, J. Catal. 130 (1991) 411.
[42] M. Shibagaki, K. Takahashi, H. Matsushita, Bull. Chem. Soc. Jpn. 61 (1988) 3283.
[43] M.A. Aramendia, V. Borau, C. Jimenez, J.M. Marinas, A. Porras, F.J. Urbano, Appl. Catal. A: Gen. 172 (1998) 31.
[44] T. Upadhya, S.P. Katdare, D.P. Sabde, V. Ramaswamy, A. Sudalai, J. Chem. Soc. Chem. Commun. (1997) 1119.